Mineralogical Magazine, December 2008, Vol. 72(6), pp. 1319–1328

Weathering microenvironments on feldspar surfaces: implications for understanding fluid-mineral reactions in soils

M. R. Lee[1,*], D. J. Brown[1], M. E. Hodson[2], M. MacKenzie[3,†] and C. L. Smith[1,§]

[1] Department of Geographical and Earth Sciences, University of Glasgow, Gregory Building, Lilybank Gardens, Glasgow G12 8QQ, UK
[2] Department of Soil Science, School of Human and Environmental Sciences, The University of Reading, Whiteknights, Reading RG6 6DW, UK
[3] Department of Physics and Astronomy, Kelvin Building, University of Glasgow, Glasgow G12 8QQ, UK

[*Received 5 November 2008; Accepted 20 February 2009*]

ABSTRACT

The mechanisms by which coatings develop on weathered grain surfaces, and their potential impact on rates of fluid-mineral interaction, have been investigated by examining feldspars from a 1.1 ky old soil in the Glen Feshie chronosequence, Scottish highlands. Using the focused ion beam technique, electron-transparent foils for characterization by transmission electron microscopy were cut from selected parts of grain surfaces. Some parts were bare whereas others had accumulations, a few micrometres thick, of weathering products, often mixed with mineral and microbial debris. Feldspar exposed at bare grain surfaces is crystalline throughout and so there is no evidence for the presence of the amorphous 'leached layers' that typically form in acid-dissolution experiments and have been described from some natural weathering contexts. The weathering products comprise sub-μm thick crystallites of an Fe-K aluminosilicate, probably smectite, that have grown within an amorphous and probably organic-rich matrix. There is also evidence for crystallization of clays having been mediated by fungal hyphae. Coatings formed within Glen Feshie soils after ~1.1 ky are insufficiently continuous or impermeable to slow rates of fluid-feldspar reactions, but provide valuable insights into the complex weathering microenvironments on debris and microbe-covered mineral surfaces.

Keywords: alkali feldspar, TEM, smectite, weathering.

Introduction

The development of clay mineral coatings is a typical outcome of feldspar weathering in soils in addition to feldspar-fluid reactions in diagenetic and hydrothermal contexts. If these coatings are sufficiently thick, continuous and impermeable, the rates of subsequent weathering reactions will be limited by slow diffusive transport of ions between the pore fluid and mineral surface (i.e. the coatings will be 'protective'). Velbel (1993) developed a model to predict whether coatings will have such a rate-limiting effect, which is based on the relative molar volumes of reactant (V_{react}) and product (V_{prod}) minerals and assuming conservative behaviour of ions such as Al. In the case of the weathering of orthoclase to gibbsite and kaolinite, the V_{prod}/V_{react} values are 0.30 and 0.46, respectively (Velbel, 1993), and as these values are <1, the coatings will not slow subsequent weathering rates. Such predictions are supported by some observations of feldspars coated with clays (e.g. Berner and Holdren, 1979; Zhu *et al.*, 2006) and Fe-rich precipitates (Hodson, 2003), although results of other investigations indicate that reaction rates may slow as weathering products accumulate on grain surfaces (Nugent *et al.*, 1998).

* E-mail: m.lee@ges.gla.ac.uk
† Present address: Institut für Mineralogie, Westfälische, Wilhelms-Universität Münster, Corrensstrasse 24, 48149 Münster, Germany
§ Present address: Department of Mineralogy, The Natural History Museum, London SW7 5BD, UK
DOI: 10.1180/minmag.2008.072.6.1319

In order to make better predictions of the potential impact of grain coatings on feldspar weathering, more information is needed on their microstructure and on their mechanisms of formation, which may include: (1) direct crystallization from solution; (2) crystallization of a previously formed amorphous precipitate (e.g. Parham, 1969; Eggleton and Buseck, 1980; Eggleton, 1987); (3) topotactic replacement of feldspar; and (4) replacement of a 'leached layer' produced by chemical weathering of feldspar (e.g. Tazaki, 1986; Kawano and Tomita, 1994). Coatings formed by mechanisms 3 and 4 would be expected to have a low porosity and permeability and a coherent interface with the feldspar grain and so will potentially have a greater impact on weathering rates than porous aggregates of clay minerals that are likely to form by mechanisms 1 and 2. Fresh impetus for exploring the microstructure of grain coatings has recently come from Zhu *et al.* (2006), who found that feldspar grains from a ~200 Ma sandstone had kaolinite-smectite coatings overlying an amorphous layer of indeterminate origin. If commonplace, such complex microstructures may be highly informative about the temporal development of weathering processes.

Here we describe results of a transmission electron microscope (TEM) investigation of the composition, microstructure and origins of weathering-product coatings on feldspar grains. The electron-transparent foils for TEM work were prepared using the focused ion beam (FIB) technique and from carefully selected parts of the surfaces of alkali feldspars extracted from a young (~1.1 ky) soil. As they are at a very early stage of weathering, the near-surface regions of these grains should record mechanisms of fluid-mineral interaction most clearly. The results of this study highlight the complexity of reactions taking place within microenvironments on rough and debris-covered grain surfaces and also help in understanding the potential role of such coatings in determining mineral weathering rates.

Methodology

Soils and their mineralogy

This study used naturally weathered feldspars from a chronosequence in Glen Feshie, a valley on the western margin of the Cairngorm massif (northeast Scotland). The chronosequence comprises soils ranging from 80 to 13,000 y in age and has developed on a series of Holocene river terraces composed of gravels derived predominantly from Proterozoic Moine schists (Robertson-Rintoul, 1986). A number of studies of temporal changes in weathering rates have used the Glen Feshie chronosequence. Bain *et al.* (1993) demonstrated that loss of base cations from these soils increases exponentially with their age and Hodson *et al.* (1998) showed that the degree of etch pitting of alkali and plagioclase feldspars is greater in the older soils. The soil studied here (sampled from National Grid Reference NN 84502 92401) supports a boreal heather moor and is a freely draining mineral alluvial soil (fluvisol) with a radiocarbon age of 1100 ± 40 y BP (Bain *et al.*, 1993). This age was derived from the organic horizon of an earlier soil that was buried during development of the river terrace and so gives only the maximum duration of mineral weathering. Bain *et al.* (1993) showed that this soil has a long term weathering rate of 55.9 mEq m^{-2} y^{-1}. Millimetre-sized feldspar grains with prominent (001) or (010) cleavage surfaces were hand picked from samples taken at depths of 2−7 cm (Ah horizon) and 18−23 cm (Bs horizon). The Ah horizon has a pH of 4.4 and the exchangeable cation values for Ca, Mg, Na and K were 2.1, 1.0, 0.08 and 0.82 mEq/100 g. The Bs horizon has a pH of 4.6 and exchangeable cation values for Ca, Mg, Na and K were 0.34, 0.26, 0.07 and 0.17 meq/100 g, respectively (Bain *et al.*, 1993). Alkali feldspars comprise 29 wt.% and 24 wt.% of soil in the Ah and C horizons (Bain *et al.*, 1993; the Bs horizon was not analysed) and are orthoclase cryptoperthites. Using scanning electron microsope (SEM) X-ray microanalysis, Hodson *et al.* (1998) described abundant Al-Si-Fe oxyhydroxide coatings on the surfaces of feldspar grains extracted from Glen Feshie soils but the only clay mineral recorded from the 1.1 ky soil, by Bain *et al.* (1993), was interstratified mica-vermiculite.

SEM, FIB and TEM

Following extraction from the soils, feldspar grains were fixed to aluminium SEM stubs using an epoxy resin (Fig. 1*a*), then sputter coated with gold. Grain surfaces were imaged using secondary electrons (SE) in a Quanta 200F field-emission SEM operated at 10−20 kV and regions with and without weathering-product coatings were selected for further study. Electron-transparent foils for TEM work were cut from various areas of grain surfaces with a FEI 200TEM single beam

FIB instrument using 30 kV Ga^+ ions. The FIB technique and its applications in Earth Science have been described by Heaney *et al.* (2001), Lee *et al.* (2003) and Wirth (2004) and so is only summarized here. A ~1 μm thick platinum strap was initially deposited over the area of interest using the Ga^+ ion beam, and then a pair of trenches was cut astride the strap to leave a ~1 μm thick slice remaining between them. Its sidewalls were 'polished' until the slice reached a thickness of ~100 nm and it was then cut free at its base and sides. The foil was lifted out using an *ex situ* micromanipulator and placed on a holey carbon film for study. Amorphization of grain surfaces by implantation of the Ga^+ ions used for imaging and platinum deposition was a significant potential problem in the present study and so, following Lee *et al.* (2007), grains were sputter coated with a thick layer of gold prior to FIB work. In a small number of cases, Ga^+ ions were still implanted because an insufficient thickness of protective gold had accumulated, but the resulting amorphous layer provided a very useful frame of reference for assessing whether a naturally formed amorphous layer could have been identified if present.

The FIB-produced foils were imaged initially by low-voltage scanning transmission electron microscopy (LV-STEM) in the Quanta SEM

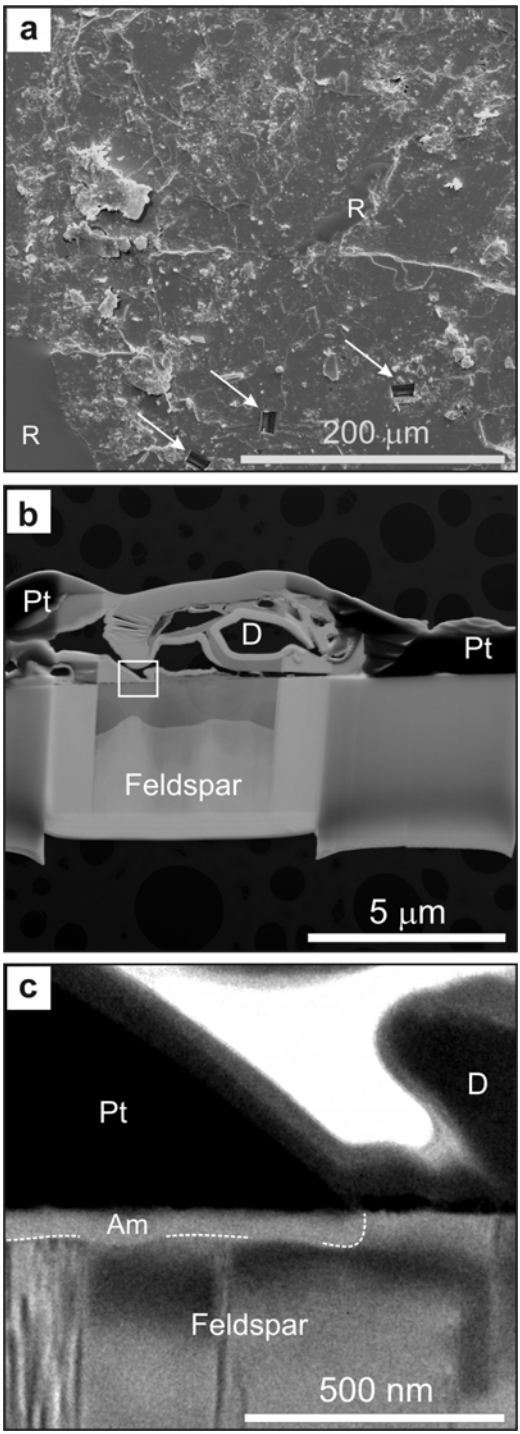

FIG. 1. Images of alkali feldspars from the Bs horizon of the 1.1 ky Glen Feshie soil. (*a*) SE SEM image of a grain surface partially coated with weathering products. Three FIB-produced trenches are indicated by arrows. The grain is mounted in resin (R). (*b*) Dark-field LV-STEM image of a foil that was cut using the FIB through an area where a diatom (D) was resting on an otherwise bare grain surface. Platinum (Pt) was deposited directly on bare areas of the grain surface (sampled by the left and right hand sides of the foil), whereas the diatom protected feldspar beneath it from platinum deposition and associated gallium implantation (sampled by the central part of the foil). (*c*) Bright-field TEM image of the boxed area in (*b*). In the middle and left hand side of the image, the bare surface is overlain directly by FIB-deposited platinum (Pt). The outermost 55 nm of this feldspar has been rendered amorphous by implantation of the Ga^+ ions used in platinum deposition. The contact between the amorphous material and feldspar is indicated by a dashed white line (labelled Am) along part of its length. On the right hand side the diatom, debris has protected the grain surface from ion implantation and the feldspar is crystalline throughout.

(Smith *et al.*, 2006; Lee and Smith, 2006) then loaded into a double-tilt holder for TEM work. Diffraction contrast imaging and selected area electron diffraction (SAED) used a FEI Tecnai T20 TEM operated at 200 kV whereas high resolution TEM (HRTEM) imaging and energy-dispersive X-ray microanalysis was undertaken on a FEI Tecnai TF20 field-emission instrument, also operated at 200 kV, and for microanalysis in STEM mode. As the foils had to be tilted typically by a couple of degrees for effective imaging (i.e. so that the electron beam is nearly parallel to a prominent zone axis), the outermost $\leqslant$2.5 nm of the feldspar grain may be obscured by the material above and below, thus imposing a ~2.5 nm limit on the minimum thicknesses of amorphous layers that could be confidently identified (Lee *et al.*, 2007).

Results

Imaging by SEM demonstrates that cleavage surfaces of most grains from the Ah and Bs horizons are partially coated by weathering products, themselves usually mixed with microbial filaments (probably fungal hyphae), microbial debris including diatom frustules, and detrital mineral grains (Fig. 1*a*). Using the FIB technique, foils were cut from the coatings and also adjacent areas of the grain surfaces that were bare (i.e. with feldspar exposed). As all cleavage surfaces studied by TEM had these coatings, we can be confident that the grains had been exposed to soil waters for a considerable length of time.

Bare grain surfaces

Areas of grain surfaces without coatings are featureless apart from shallow steps and occasional etch pits. As the potential presence of amorphous 'leached layers' immediately beneath the grain surface was an important consideration in the present study, our ability to identify such layers using the FIB-TEM technique was tested by undertaking the following experiment. A grain was sputter coated with a very thin layer of gold and a foil was cut using the FIB from a carefully selected area of the grain surface, part of which was bare and part of which was overlain by a diatom frustule (Fig. 1*b*). Imaging by TEM of the foil showed that in areas where platinum had been deposited by the Ga^+ ion beam directly onto the bare grain surface the feldspar had been rendered amorphous to a depth of ~55 nm (Fig. 1*c*); the gold coat was of insufficient thickness to be protective. As this FIB-produced amorphous layer could be readily identified by TEM diffraction contrast imaging, we conclude that the same technique could be used to find naturally formed amorphous layers if present. Areas of the grain surface that were protected from Ga^+ ion implantation by the overlying frustule were found by TEM imaging to be crystalline throughout (Fig. 1*c*) and so, if present, any amorphous layer must be less than the thickness that can be resolved in slightly tilted foils (i.e. <2.5 nm). Imaging by TEM of foils cut from bare areas of other grain surfaces (which had been protected from Ga^+ ion implantation during FIB work using a thicker gold coat), confirmed that naturally formed amorphous layers were undetectable.

Coated grain surfaces

In cross-section, the grain coatings are a few micrometres thick and laminated on the tens to hundreds of nanometre scale (Figs 2*a*,*b*). The weathering products are predominantly amorphous

FIG. 2 (*facing page*). Images of foils cut from the (001) surfaces of alkali feldspars from the Bs horizon of the 1.1 ky Glen Feshie soil. (*a*) SE image taken prior to lift-out of a foil that has been cut through an accumulation of weathering products containing debris including diatom frustules. (*b*) Bright-field TEM image of the foil showing feldspar (featureless) that is overlain by laminated weathering products (WP). The protective gold (Au) and platinum (Pt) are labelled. (*c*) High-resolution TEM image of the amorphous weathering products in (*b*) showing a crystalline ribbon with a ~1 nm basal layer spacing. (*d*) HRTEM image of the interface between feldspar and amorphous weathering products. The faint lattice planes immediately above the feldspar (between the dashed white lines) are suggestive of a ~1–2 nm thick gradational contact with the weathering products, but could equally be an artifact of imaging through a slightly tilted grain surface, or delocalization of information. Electron beam near [100]. (*e*) Dark-field LV-STEM image of a foil cut through fungal hyphae (F) lying on an otherwise bare grain surface. The feldspar is featureless apart for a few micropores. The protective gold (Au) and platinum (Pt) are labelled. (*f*) HRTEM image of the boxed area in (*e*), which is in the lower part of a hypha and contains a crystallite with a ~1.4 nm basal layer spacing.

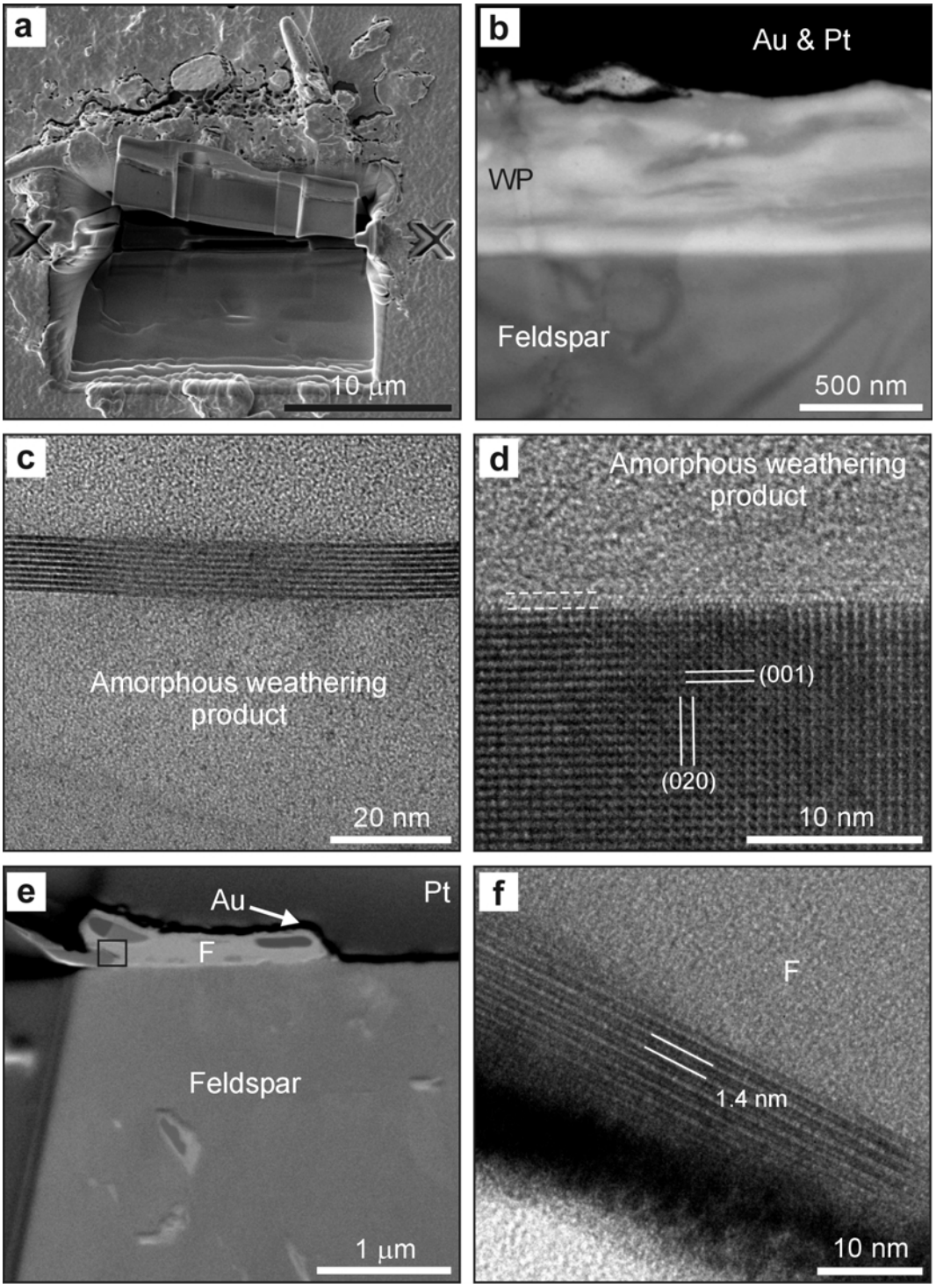
a
10 μm
b
Au & Pt
WP
Feldspar
500 nm
c
Amorphous weathering product
20 nm
d
Amorphous weathering product
(001)
(020)
10 nm
e
Au
Pt
F
Feldspar
1 μm
f
F
1.4 nm
10 nm

but contain crystalline ribbons which are a few nm thick (Fig. 2*c*), the presence of which helps to define the lamination observed at lower magnifications (Fig. 2*b*). Lattice fringes within these ribbons have a basal layer spacing of ~1.0–1.2 nm and lie approximately parallel to the outer surface of the feldspar grain (Fig. 2*c*). The TEM X-ray microanalysis shows that the amorphous material is

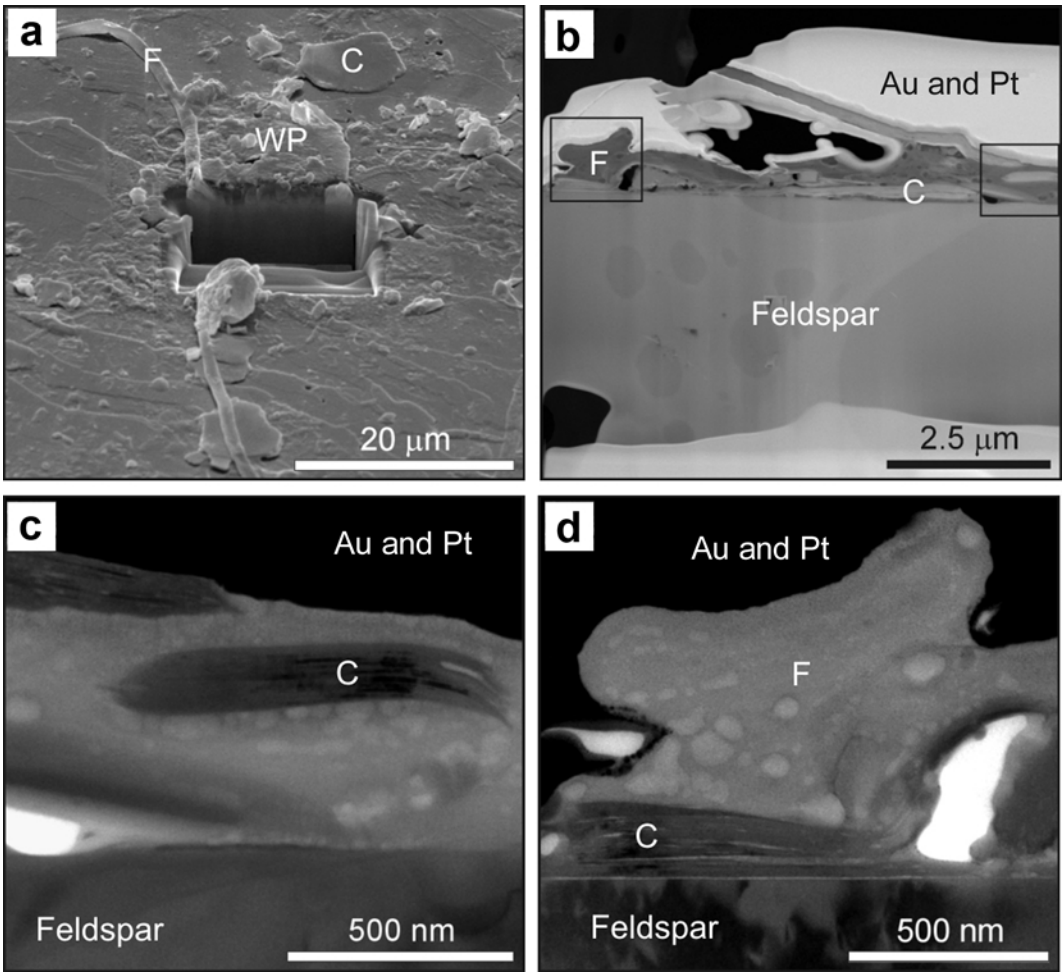

FIG. 3. Images of the (001) cleavage surface of an alkali feldspar from the Ah horizon of the 1.1 ky Glen Feshie soil. (*a*) SE image of the grain tilted at 50º away from the viewer and after lift-out of a FIB-produced foil. The feldspar surface has shallow steps and is partly overlain by structureless weathering products (WP), discrete clay mineral crystals (C) and fungal hyphae (F). (*b*) Dark-field LV-STEM image of most of the foil. The feldspar is featureless and gold (Au) and platinum (Pt) coatings are labelled. The prominent fungal hypha (F) in (a) is clearly defined, as are the clay mineral crystals (C). Between the clays are some sub-micrometre sized detrital grains of feldspar and a matrix that has a lower mean atomic number (and so is darker grey) than the feldspar and clays. (*c*) Bright-field TEM image of the boxed area on the right hand edge of (*b*). A small clay crystal (C) is supported within a vesicular matrix. Note the fine-scale interdigitation of the clay with matrix on its right hand side. Electron beam near feldspar [100]. (*d*) Bright-field TEM image of the boxed area on the left hand edge of (*b*). A fungal hypha (F) overlies a clay crystal (C), itself resting on strongly diffracting feldspar. The ~5 nm thick non-diffracting band between the feldspar and clay lies above the current grain surface and has not been formed by amorphization of feldspar. Electron beam parallel to feldspar [100].

C- and O-rich with varied concentrations of Si, Fe and K, whereas the crystalline ribbons are aluminosilicates often containing K and Fe. The interface between feldspar and the amorphous coating is typically sharp, although one high-resolution image shows faint lattice planes with a spacing equivalent to orthoclase (001) within the weathering products (Fig. 2*d*). This apparently gradational interface may be indicative of incipient replacement of the feldspar, but is more likely to be an artifact of delocalization of the information, which is a problem with high-resolution imaging using a field emission TEM. A number of foils were also from fungal hyphae that cross-cut otherwise bare areas of grain surfaces (Fig. 2*e*). Crystallites with a ~1.4 nm basal layer spacing were found in close association with one of these hyphae (Fig. 2*f*).

Some areas of the grain surface host more coarsely crystalline clays (Figs 3*a,b*) the constituent crystals of which are <~100 nm thick and have basal layer spacings of ~1.0–1.4 nm (average ~1.2 nm), as measured from HRTEM images and SAED patterns (Fig. 3*b–d*). A vesicular and amorphous matrix is often present between these crystals and the fine-scale interfingering of the two constituents of the coatings suggests that the clays have crystallized *in situ* (Fig. 3*c*). The interface of clay crystals with the outermost part of the feldspar grain is sharp on the nanometer scale (Fig. 3*d*). Fungal hyphae have a similar vesicular appearance to the amorphous matrix in the TEM images, although some vestiges of biological ultrastructure remain (Fig. 3*d*). X-ray microanalysis shows that in contrast to the feldspar substrate (Fig. 4*a*) the amorphous material consists mainly of C, O and Si with traces of Al, K and Fe (Fig. 4*b*). The clays are Fe-aluminosilicates with traces of Mg, K and occasionally Ti (Fig. 4*c,d*) and when taken together with lattice spacings, this composition is consistent with smectite.

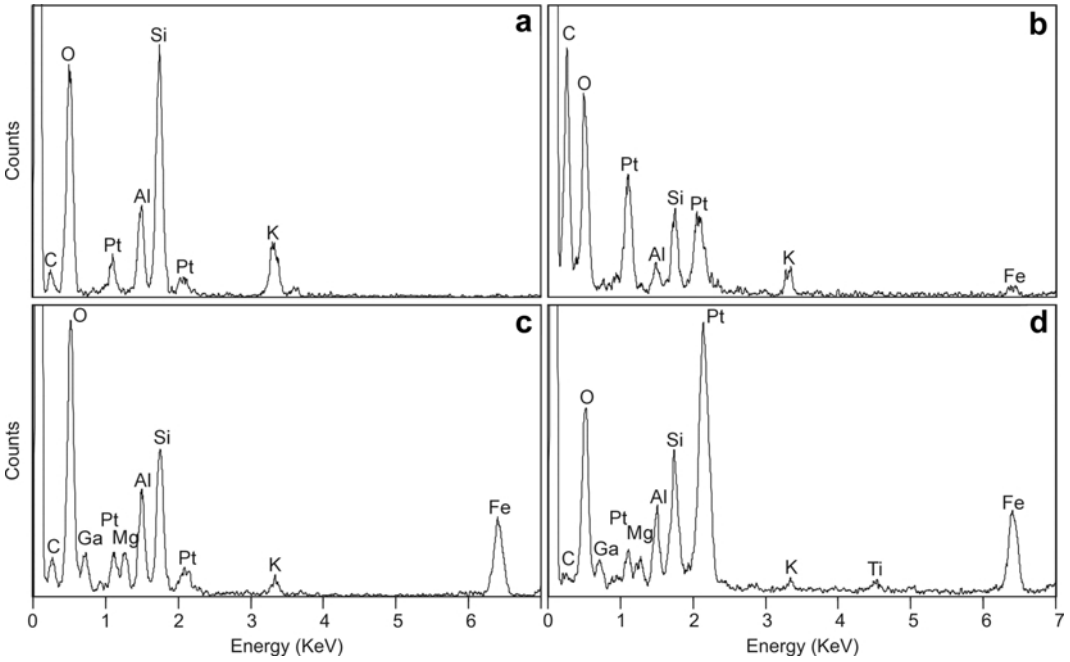

FIG. 4. X-ray spectra of the alkali feldspar grain and associated weathering products in Fig. 3. The spectra were obtained from small areas of the foil over which the electron beam was rastered with the Tecnai F20 operated in STEM mode. Gallium in these spectra was implanted during ion milling and the Pt is from the FIB-deposited protective strap. (*a*) The outermost part of the alkali feldspar (150 nm × 210 nm raster). (*b*) Amorphous weathering products (100 nm × nm raster). (*c*) Clay mineral crystal in the middle of Fig. 3*c* (100 nm × 140 nm nm raster). (*d*) Clay mineral crystal in the top left of Fig. 3*c* and immediately beneath the platinum strap (140 nm × 190 nm raster).

Discussion

The aims of this study were to characterize the surfaces of feldspars from a young soil in order to determine the mechanism(s) of formation of any coatings present and so infer their potential impact on subsequent weathering. Previous work has shown that mineral weathering is active in all soils from the Glen Feshie chronosequence (Bain *et al.*, 1993), and the etched and coated grains examined in this study have also clearly had considerable exposure to soil waters. The degree of chemical weathering of the feldspar is difficult to quantify using SEM or TEM observations, but can be estimated from previously determined rate data. The compilation of weathering data in White and Brantley (2003) indicates that the dissolution rate of K-feldspar after 1.1 ky will be between 10^{-14} and 10^{-15} moles m^{-2} s^{-1}. If constant throughout the 1.1 ky history of the soil, this rate corresponds to removal of a few tens of nanometres from grain surfaces over 1.1 ky, assuming that all parts of the grains dissolve at equal rates. This value is consistent with the degree of etch pitting observed by SEM.

First we ask if the weathering-product coatings could have formed by replacement of feldspar or a chemically modified 'leached layer' (i.e. mechanisms 3 and 4 outlined in the Introduction). Topotactic replacement is a key process by which chain silicates naturally weather to clays (e.g. Banfield and Barker, 1994; Banfield *et al.*, 1995) and, owing to the coherent interstratification of primary minerals with their reaction products, rates of subsequent weathering may be slowed significantly (Banfield and Barker, 1994). With regard to the Glen Feshie feldspars, smectite (001) lies approximately parallel to orthoclase (001) (Figs 2*c*, 3*d*) but despite this orientation relationship there is no evidence for *in situ* recrystallization of orthoclase to smectite (e.g. nowhere do the two minerals show a fine-scale interstratification). Leached layers are a characteristic by-product of feldspar dissolution under acid laboratory conditions whereby selective removal of Al and Na/K/Ca relative to Si, renders the outermost <0.1 μm of grains amorphous and non-stoichiometric (e.g. Casey *et al.*, 1989; Muir *et al.*, 1989; Hellmann *et al.*, 1990). Kawano and Tomita (1994) found that a tens of nm thick leached layer on albite grains hydrothermally reacted with distilled water had subsequently crystallized to Na-smectite and mica *via* a non-crystalline and fibrous material. Tazaki (1986) described comparable processes during natural weathering of microcline perthites from Brazil whereby 'primitive-clay precursors' were inferred to have been produced by crystallization of a leached layer. However, it is currently unclear whether leached layers can form during natural weathering of K-feldspars, even in quite acidic soils (Lee *et al.*, 2007, 2008) and FIB-TEM results from the Glen Feshie feldspars show that if present, any layers of amorphous feldspar must be <2.5 nm thick. This conclusion is consistent with the <2 nm thickness of leached layers found on feldspars used in dissolution experiments undertaken at pH values similar to those in the Glen Feshie soil (Blum, 1994). We therefore conclude that leached layers are either absent from grains in the 1.1 ky soil, or, if present, <2.5 nm thick, and so could not have played any significant role in formation of the much thicker coatings observed.

In the absence of evidence for a replacive origin, the coatings must have precipitated from solution and the presence of Mg, Ti and Fe in the smectite indicates considerable mobility of ions within soil waters. The FIB-produced foils show that even the relatively coarsely crystalline weathering products are interstratified with an amorphous matrix (Fig. 3c) indicating that most if not all of the clays observed formed from a non-crystalline precursor. All stages in the crystallization of these precursors have been observed, from the formation of ribbons a few nanometres thick (Fig. 2*c*) to platy crystals which are hundreds of nm in size (Fig. 3*c*). Amorphous weathering products have been widely described previously and are interpreted to be an intermediate stage between weathering of soil aluminosilicates and crystallization of clays. These Al-Si-Fe oxyhydroxide gels typically have a porous cell-textured, foam- or ring-like morphology and a proto-crystalline structure (e.g. Eggleton and Buseck, 1980; Eggleton, 1987; Tazaki and Fyfe, 1987; Banfield and Eggleton, 1990; Kawano and Tomita, 1996). With time, this material can be replaced by clays, for example a K-Ca-Fe smectite in the case of granodiorite weathering in Australia (Banfield and Eggleton, 1990). Comparable transformations of amorphous Al-Si-Fe oxyhydroxides to ribbons of Fe-rich smectite (with a 1.0−1.3 nm basal layer spacing) have been described from a Jurassic stromatolite using TEM (Sanchez-Navas *et al.*, 1998). In this case, the amorphous material was formed from an extracellular bacterial gel and the smectite crystallized during early diagenesis. The C-rich composition of the amorphous precursors

to clays in the Glen Feshie coatings is suggestive of an organic involvement in mineralization, and this assumption is supported by the direct association of nanoscale crystallites with fungal hyphae that cross-cut otherwise bare grain surfaces (Fig. 2*f*).

These observations demonstrate the complexity of precipitation and crystallization reactions taking place on feldspar grain surfaces during early stages of weathering, but can the coatings produced slow subsequent rates of fluid-mineral reaction? The Glen Feshie coatings are considerably more compact and have a lower porosity, and presumably permeability, than the protocrystalline weathering products described previously and so may be expected to have a greater impact on rates of aqueous diffusion between soil waters and the mineral surface. However, in the 1.1 ky soil at least we suggest that, these coatings are of insufficient thickness or abundance to limit rates of feldspar weathering.

Conclusions

This study has highlighted the importance of amorphous precipitates on weathered grain surfaces as precursors to clay mineral crystallization, and has provided direct evidence for microbial mediation of clay growth. We have also shown that the FIB-TEM technique is a powerful tool for the characterization of precipitation and crystallization reactions taking place within microenvironments on debris-covered feldspar substrates, which have until now been very difficult to study using conventional imaging and analysis techniques. Although coatings on grains in the young Glen Feshie soils are insufficiently well developed to impact upon rates of weathering, they offer an important tool that can be used for elucidating mechanisms and even rates of fluid-mineral reactions.

Acknowledgements

The authors are grateful to Professor Alan Craven (Physics and Astronomy, Glasgow University) for access to the FIB and TEM facilities, Billy Smith and Colin How for their technical assistance and to Roland Hellmann for illuminating discussions. They also thank Katharina Hartmann and Sue Brantley for their helpful reviews, which have improved this manuscript. This research was supported by the UK NERC.

References

Bain, D.C., Mellor, A., Robertson-Rintoul, M.S.E. and Buckland, S.T. (1993) Variations in weathering processes and rates with time in a chronosequence of soils from Glen Feshie, Scotland. *Geoderma*, **57**, 275–293.

Banfield, J.F. and Barker, W.W. (1994) Direct observation of reactant-product interfaces formed in natural weathering of exsolved, defective amphibole to smectite: Evidence for episodic, isovolumetric reactions involving structural inheritance. *Geochimica et Cosmochimica Acta*, **58**, 1419–1429.

Banfield, J.F. and Eggleton, R.A. (1990) Analytical transmission electron microscope studies of plagioclase, muscovite and K-feldspar weathering. *Clays and Clay Minerals*, **38**, 77–89.

Banfield, J.F., Ferruzzi, G.G., Casey, W.H. and Westrich, H.R. (1995) HRTEM study comparing naturally and experimentally weathered pyroxenoids. *Geochimica et Cosmochimica Acta*, **59**, 19–31.

Berner, R.A. and Holdren, G.R. (1979) Mechanism of feldspar weathering. 2. Observations of feldspars from soils. *Geochimica et Cosmochimica Acta*, **43**, 1173–1186.

Blum, A.E. (1994) Feldspars in weathering. Pp. 595–630 in: *Feldspars and their Reactions* (I. Parsons, editor), Kluwer, Dordrecht, The Netherlands.

Casey, W.H., Westrich, H.R., Massis, T., Banfield, J.F. and Arnold, G.W. (1989) The surface of labradorite feldspar after acid hydrolysis. *Chemical Geology*, **78**, 205–218.

Eggleton, R.A. (1987) Noncrystalline Fe-Si-Al oxyhydroxides. *Clays and Clay Minerals*, **35**, 29–37.

Eggleton, R.A. and Buseck, P.R. (1980) High resolution electron microscopy of feldspar weathering. *Clays and Clay Minerals*, **28**, 173–178.

Heaney, P.J., Vicenzi, E.P., Giannuzzi, L.A. and Livi, K.J.T. (2001) Focused ion beam milling: A method of site-specific sample extraction for microanalysis of Earth and planetary materials. *American Mineralogist*, **86**, 1094–1099.

Hellmann, R., Eggleton, C.M., Hochella Jr., M.F. and Crerar, D.A. (1990) The formation of leached layers on albite surfaces during dissolution under hydrothermal conditions. *Geochimica et Cosmochimica Acta*, **54**, 1267–1281.

Hodson, M.E. (2003) The influence of Fe-rich coatings on the dissolution of anorthite at pH 2.6. *Geochimica et Cosmochimica Acta*, **67**, 3355–3363.

Hodson, M.E., Langan, S.J., Kennedy, F.M. and Bain, D.C. (1998) Variation in soil surface area in a chronosequence of soils from Glen Feshie, Scotland and its implications for mineral weathering rate calculations. *Geoderma*, **85**, 1–18.

Kawano, M. and Tomita, K. (1994) Growth of smectite

from leached layer during experimental alteration of albite. *Clays and Clay Minerals*, **42**, 7–17.

Kawano, M. and Tomita, K. (1996) Amorphous aluminium hydroxide formed at the earliest weathering stages of K-feldspar. *Clays and Clay Minerals*, **44**, 672–676.

Lee, M.R. and Smith, C.L. (2006) Scanning transmission electron microscopy using a SEM: Applications to mineralogy and petrology. *Mineralogical Magazine*, **70**, 579–590.

Lee, M.R., Bland, P.A. and Graham, G. (2003) Preparation of TEM samples by focused ion beam (FIB) techniques: applications to the study of clays and phyllosilicates in meteorites. *Mineralogical Magazine*, **67**, 581–592.

Lee, M.R., Brown, D.J., Smith, C.L., Hodson, M.E., MacKenzie, M. and Hellmann, R. (2007) Characterisation of mineral surfaces using FIB and TEM: A case study of naturally-weathered alkali feldspars. *American Mineralogist*, **92**, 1383–1394.

Lee, M.R., Hodson, M.E., Brown, D.J., MacKenzie, M. and Smith, C.L. (2008) The composition and crystallinity of the near-surface regions of weathered alkali feldspars. *Geochimica et Cosmochimica Acta*, **72**, 4962–4975.

Muir, I.J., Bancroft, G.M. and Nesbitt, H.W. (1989) Characteristics of altered labradorite surfaces by SIMS and XPS. *Geochimica et Cosmochimica Acta*, **53**, 1235–1241.

Nugent, M.A., Brantley, S.L., Pantano, C.G. and Maurice, P.A. (1998) The influence of natural mineral coatings on feldspar weathering. *Nature*, **395**, 588–591.

Parham, W.E. (1969) Formation of halloysite from feldspar: low temperature artificial weathering versus natural weathering. *Clays and Clay Minerals*, **17**, 13–22.

Robertson-Rintoul, M.S.E. (1986) A quantitative soil-stratigraphic approach to the correlation and dating of post-glacial river terraces in Glen Feshie, western Cairngorms. *Earth Surface Processes Landforms*, **11**, 605–617.

Sanchez-Navas, A., Martin-Algarra, A. and Nieto, F. (1998) Bacterially-mediated authigenesis of clays in phosphate stromatolites. *Sedimentology*, **45**, 519–533.

Smith, C.L., Lee, M.R. and MacKenzie, M. (2006) New opportunities for nanomineralogy using FIB, STEM/EDX and TEM. *Microscopy Analysis*, **111**, 17–20.

Tazaki, K. (1986) Observation of primitive clay precursors during microcline weathering. *Contributions to Mineralogy and Petrology*, **92**, 86–88.

Tazaki, K. and Fyfe, W.S. (1987) Primitive clay precursors formed on feldspar. *Canadian Journal Earth Science*, **24**, 506–527.

Velbel, M.A. (1993) Formation of protective surface layers during silicate mineral weathering under well leached oxidizing conditions. *American Mineralogist*, **78**, 405–414.

White, A.F. and Brantley, S.L. (2003) The effect of time on the weathering of silicate minerals: why do weathering rates differ in the laboratory and field? *Chemical Geology*, **202**, 479–506.

Wirth, R. (2004) Focused Ion Beam (FIB): A novel technology for advanced application of micro- and nanoanalysis in geosciences and applied mineralogy. *European Journal of Mineralogy*, **16**, 863–876.

Zhu, C., Veblen, D.R., Blum, A.E. and Chipera, S.J. (2006) Naturally weathered feldspar surfaces in the Navajo Sandstone aquifer, Black Mesa, Arizona: Electron microscopic characterization. *Geochimica et Cosmochimica Acta*, **65**, 3459–3474.